Formation of apatite oxynitrides by the reaction between apatite-type oxide ion conductors, La8+xSr2-x(Si/Ge)6O26+x/2, and ammonia

Orera, Alodia; Headspith, D; Apperley, DC; Francesconi, MG; Slater, Peter

DOI:
10.1016/j.ssc.2009.09.029
10.1016/j.jssc.2009.09.029

Formation of apatite oxynitrides by the reaction between apatite-type oxide ion conductors, $La_{8+x}Sr_{2-x}(Si/Ge)_6O_{26+x/2}$, and ammonia

A. Orera[1], D. Headspith[2], D.C. Apperley[3], M.G. Francesconi[2], and P.R. Slater[1*]

[1] School of Chemistry, University of Birmingham, Birmingham B15 2TT. UK

[2] Department of Chemistry, The University of Hull, Cottingham Road, Hull. UK

[3] Department of Chemistry, Durham University, South Road, Durham. DH1 3LE. UK.

[*]Correspondence to:

Dr. P.R. Slater

School of Chemistry, University of Birmingham, Birmingham B15 2TT. UK

Tel. +44 (0)121 4148906

Fax +44 (0)121 4144403

p.r.slater@bham.ac.uk

Abstract

Following growing interest in the use of ammonia as a fuel in Solid Oxide Fuel Cells (SOFCs), we have investigated the possible reaction between the apatite silicate/germanate electrolytes, $La_{8+x}Sr_{2-x}(Si/Ge)_6O_{26+x/2}$, and NH_3 gas. We examine how the composition of the apatite phase affects the reaction with ammonia. For the silicate series, the results showed a small degree of N incorporation at 600°C, while at higher temperatures (800°C), substantial N incorporation was observed. For the germanate series, partial decomposition was observed after heating in ammonia at 800°C, while at the lower temperature (600°C), significant N incorporation was observed. For both series, the N content in the resulting apatite oxynitride was shown to increase with increasing interstitial oxide ion content (x) in the starting oxide. The results suggest that the driving force for the nitridation process is to remove the interstitial anion content, such that for the silicates the total anion (O+N) content in the oxynitrides approximates to 26.0, the value for an anion stoichiometric apatite. For the germanates, lower total anion contents are observed in some cases, consistent with the ability of the germanates to accommodate anion vacancies. The removal of the mobile interstitial oxide ions on nitridation suggests problems with the use of apatite-type electrolytes in SOFCs utilising NH_3 at elevated temperatures.

Keywords: Apatite, ammonia, solid oxide fuel cell

Introduction

The worldwide concerns regarding diminishing fossil fuel reserves and increasing greenhouse gas emissions has given fuel cell research considerable impetus. The traditionally favoured fuel for such devices is hydrogen, since the only emission from the fuel cell is then water. However, hydrogen has a number of problems, with particular concerns regarding strategies for efficient storage and transportation. Therefore, other potential fuels have started to attract significant attention, with one example being ammonia. Among the benefits of ammonia are that it is easy to store as a liquid and would simply produce N_2 and H_2O in terms of emissions in a fuel cell. Consequently a number of researchers have investigated the operation of solid oxide fuel cells with NH_3 as the fuel, with promising results obtained [1-6]. However, the use of NH_3 in place of H_2 raises other questions, in particular the possibility that nitridation may occur on the anode side of the cell under operating conditions. Indeed recent research has shown evidence for significant nitridation of CeO_2 and the apatite-type oxide ion conductor $La_{9.33}Si_6O_{26}$ on heating in NH_3 [7, 8]. In this paper, we extend our earlier work on heat treatment of $La_{9.33}Si_6O_{26}$ in NH_3 to other apatite-type oxide ion conductors, $La_{8+x}Sr_{2-x}(Si/Ge)_6O_{26+x/2}$, to examine what influence the composition, in particular the oxygen content, has on the process.

Apatite-type silicates/germanates, $(Ln/A)_{10-x}(Si/Ge)_6O_{26+y}$ (Ln=rare earth, A=alkaline earth), have been attracting considerable interest as a new class of oxide-ion conducting electrolytes [9-42]. Their structure may be described in terms of an $(Ln/A)_{4-x}(Si/GeO_4)_6$ framework, with the remaining $(La/A)_6O_2$ units accommodated in the channels within the

framework. In these systems, the oxide ion conduction process has been shown to proceed via a mechanism involving interstitial oxide ions, which are present as a result of either oxygen hyperstoichiometry (x>0) in $La_{8+x}Sr_{2-x}(Si/Ge)_6O_{26+x/2}$ or Frenkel-type disorder [12-18, 21, 25-27]. Thus the conductivities of fully stoichiometric samples, e.g. $La_8Sr_2(Si/Ge)_6O_{26}$, are low, while compositions containing either oxygen excess, e.g. $La_9Sr(Si/Ge)_6O_{26.5}$, or cation vacancies, e.g. $La_{8.67}Sr(Si/Ge)_6O_{26}$, have high conductivities. With regard to the location of the interstitial oxide ions, computer modelling studies have predicted that for the silicates the most favourable interstitial oxide ion site is at the periphery of the oxide ion channels neighbouring the SiO_4 groups, which has been supported by neutron diffraction, ^{29}Si NMR, and Raman studies [14, 15, 17, 27, 36]. For the germanates, both modelling and neutron diffraction studies also indicate an interstitial position neighbouring the GeO_4 tetrahedra, although in this case the interstitial oxide ion is more closely associated, leading to five coordinate Ge [21, 26].

In our previous work on the high temperature reaction of $La_{9.33}Si_6O_{26}$ with NH_3 we showed that the level of nitridation increased with increasing temperature (600-950°C), with negligible nitridation at lower temperature, while substantial nitridation, coupled with Si loss, was observed at the highest temperature (950°C) examined. Structural (neutron diffraction, ^{29}Si NMR) data for the sample heated at 950°C in NH_3 showed no evidence for the presence of interstitial oxide ions, but rather the partial replacement of O by N (3 O^{2-} replaced by $2N^{3-}$) leads to a reduction in the total anion content, and hence anion vacancies. Considering the importance of interstitial oxide ions to the conductivity of these materials, the work hence suggested that nitridation would be detrimental to the conductivity. Following on from the large nitridation and Si loss at very high

temperatures (>800°C), the reaction with ammonia for the apatite series, $La_{8+x}Sr_{2-x}(Si/Ge)_6O_{26+x/2}$, studied here, has been limited to temperatures ≤800°C.

Experimental

A series of samples, $La_{8+x}Sr_{2-x}Si_6O_{26+x/2}$ ($0 \leq x \leq 1$) and $La_{8+x}Sr_{2-x}Ge_6O_{26+x/2}$ ($0 \leq x \leq 2$), were prepared from high purity La_2O_3, $SrCO_3$, SiO_2, and GeO_2, which were intimately mixed in the correct molar ratios and heated to 1300°C (Si) and 1100°C (Ge) for 14 hours, reground and then reheated to 1400°C (Si) and 1100°C (Ge) for a further 14 hours. For the germanates, a subsequent final heat treatment at 1300°C for 2 hours was employed. Phase purity was established through X-ray powder diffraction (Panalytical X'Pert Pro diffractometer, Cu $K\alpha_1$ radiation). The powder samples were then heated in flowing NH_3 gas (14 lt/hr) for 12 hours at temperatures of 600 and 800°C.

The N contents were determined through thermogravimetric analysis (TA instruments SDT 600/ Netzsch STA 449 thermal analysers). The samples were heated in oxygen at 10°C/min to 1000°C to convert the oxynitride back to the oxide. This leads in an increase in mass, since $3O^{2-}$ will replace $2N^{3-}$, and from the mass change observed the N content could then be determined.

^{29}Si NMR data for $La_{8+x}Sr_{2-x}Si_6O_{26+x/2}$ samples after heating in NH_3 at 800°C were recorded using a Varian Unity Inova spectrometer operating at 59.56 MHz. A direct-polarisation experiment was used with recycle delays of 5s (x=1), 10s (x=0.5), 60s (x=0). Chemical shifts are quoted relative to tetramethylsilane.

Results and discussion

For the silicate series, $La_{8+x}Sr_{2-x}Si_6O_{26+x/2}$, X-ray diffraction showed that the samples were single phase before and after NH_3 treatment (figure 1). The thermal analysis results indicated a small degree of nitridation at 600°C, with a higher temperature (800°C) required to give high levels of nitridation. For the fully stoichiometric (x=0) composition, there was negligible nitridation observed, while for the samples containing oxygen interstitials (x=0.5, 1.0) significant nitridation was observed, the level of which increased with increasing interstitial oxide ion content in the starting sample (table 1, figure 2). The calculated compositions at 800°C indicate that the final anion content (O+N) is very close to 26 for all samples, suggesting that the driving force for nitridation is the reduction in interstitial anion content. For the lower temperature (600°C) heat treatment, lower levels of N were found leading to the samples still having total anion content >26.0, thus indicating that the nitridation process was not complete.

In order to gain information about the location of the N in the structure, ^{29}Si NMR data were measured for the $La_{8+x}Sr_{2-x}Si_6O_{26+x/2}$ samples after heating at 800°C in ammonia. These data showed significant differences compared to data for the starting materials. In particular, previous work has shown that for the series, $La_{8+x}Sr_{2-x}Si_6O_{26+x/2}$, the ^{29}Si NMR spectrum for x=0 has a single peak at δ≈-77 ppm, while for x>0, a second peak is observed at δ≈-80 ppm, attributed to a silicate unit neighbouring an interstitial site [17,27]. In contrast the nitrided samples showed no evidence for this second peak in the sample with x=0.5, while for the x=1 sample, the peak intensity was greatly reduced (figure 3). This would indicate loss of the interstitial oxide ions, consistent with nitridation resulting in a lower total anion content. The x=1 sample also had some

additional weak signal at δ≈-73.5 ppm consistent with the presence of a small amount of $[SiO_3N]^{5-}$. Due to the low intensity and closeness to the main peak, accurate intensity information could, however, not be obtained. However, the absence of any signal due to $[SiO_3N]^{5-}$ in the x=0.5 phase, coupled with the very low intensity of $[SiO_3N]^{5-}$ signal in the x=1 phase, would suggest that the N has a preference for the channel anion site (figure 4), as observed in our previous study of nitridation of $La_{9.33}Si_6O_{26}$ [8].

For the germanate series, all samples showed evidence for partial decomposition after heating in NH_3 at 800°C, although the samples were stable at lower temperatures (600°C). For this series, the as-prepared samples, $La_{8+x}Sr_{2-x}Ge_6O_{26+x/2}$, are hexagonal for x≤1, while for higher oxygen excess, x>1.0, a triclinic cell is observed [25, 31]. After treatment in NH_3 gas, X-ray diffraction indicated that all samples were hexagonal. The change of symmetry (triclinic→hexagonal) for the high oxygen excess samples (figure 5) is interesting. Previous work has shown that the triclinic distortion arises from a size mismatch between the $(La/A)_{4-x}(GeO_4)_6$ (A=alkaline earth) framework and the $(La/A)_6O_2$ units due to the presence of interstitial oxide ions within the framework [21, 25, 30, 35, 43]. The increase in symmetry after heat treatment in NH_3 gas is therefore consistent with nitridation leading to a reduction in anion content, and hence loss of these interstitial oxide ions. In order to determine the level of nitridation, thermal analysis was performed, which indicated an increase in N content on increasing starting oxygen content (table 2, figure 6), as for the silicate series. In this case, however, some of the samples (e.g. x=1) showed total anion contents significantly lower than 26.0, consistent with the ability of the apatite germinates to accommodate a certain degree of oxide ion vacancies [31]. In addition, the variation of N content with x appears to involve a change in slope at x=1.0

(figure 6). Thus at low values of x, there is a sharp increase in N content with increasing x, while for x≥1.0, the slope becomes more shallow. The compositions of the samples with x≥1.0 all have oxygen contents of ≈ 24.0, which most likely indicates non-nitrided Ge (i.e. $(GeO_4)_6$), suggesting that the N is located in the channel sites as for the silicates. The instability of the germanates at higher temperatures (800°C) may, thus, be related to the beginning of nitridation of the tetrahedral sites.

In line with our previous study of the effect of NH_3 heat treatment on the apatite $La_{9.33}Si_6O_{26}$, the loss of interstitial oxide ions is expected to mean that nitridation would be detrimental to the conductivity. This is difficult to measure experimentally, since, as shown in the previous $La_{9.33}Si_6O_{26}$ study, treatment of sintered pellets (dense, low surface area) rather than powder samples leads to a reduced level of nitridation. This is consistent with the slow kinetics of N incorporation into the structure, due to poor conduction of the oxynitride, such that only the surface of the pellet is affected. The slow kinetics of nitrogen incorporation is a common feature in the literature synthesis of mixed metal oxynitrides, e.g. $LaMO_2N$ (M=Ti, Zr). Such studies invariably utilise high surface area precursors formed by soft chemistry routes to accelerate the reaction with NH_3 [44].

Overall the work would, however, suggest that the use of apatite-type electrolytes in a fuel cell operated in NH_3 would lead to problems, particularly for the germanate apatites, which show high levels of nitridation even at 600°C. In particular, partial nitridation of the surface of the anode side of the electrolyte would be expected, while the anode would undergo more nitridation similar to the powder samples studied here, since this is conventionally a high surface area Ni/electrolyte cermet. Both these factors might be expected to be detrimental to performance.

Conclusions

Heat treatment of the apatite-type electrolytes, $La_{8+x}Sr_{2-x}(Si/Ge)_6O_{26+x/2}$ ($0 \leq x \leq 2$) in ammonia gas at elevated temperatures ($\geq 600^{\circ}C$) is shown to result in substantial nitridation of the electrolyte for $x>0$ leading to a novel series of apatite-type oxynitrides. The level of nitridation increases with increasing interstitial oxide ion content in the starting apatite oxide, as the driving force appears to be the removal of these interstitial oxide ion defects. ^{29}Si NMR data suggests that the N is predominantly located in the channel anion sites.

Acknowledgements

We would like to thank EPSRC for funding (grant EP/F015178/1). We would also like to thank the EPSRC Solid State NMR Service (Durham) for the collection of NMR data. The Netzsch thermal analyser used in this research was obtained through the Science City Advanced Materials project: Creating and Characterising Next generation Advanced Materials project, with support from Advantage West Midlands (AWM) and part funded by the European Regional Development Fund (ERDF)

References

1. L. Pelletier, A. McFarlan, N. Maffei; J. Power Sources 145 (2005) 262

2. N. Maffei, L. Pelletier, J.P. Charland, A. McFarlan; J. Power Sources 140 (2005) 264

3. A. McFarlan, L. Pelletier, N. Maffei; J. Electrochem. Soc. 151 (2004) A930

4. J. Staniforth, R.M. Ormerod; Green Chemistry 5 (2003) 606

5. G. Meng, G. Ma, Q. Ma, R. Peng, X.Lui; Solid State Ionics 178 (2007) 697

6. K. Xie, G. Ma, B. Lin, Y. Jiang, J. Gao, X. Liu, G. Meng; J. Power Sources 170 (2007) 38.

7. A. Belen-Jorge, J. Fraxedas, A. Cantarero, A.J. Williams, J. Rogers, J.P. Attfield, A. Fuertes; Chem. Mater. 20 (2008) 1682.

8. E. Kendrick, D. Headspith, A. Orera, D.C. Apperley, R.I. Smith, M.G. Francesconi, P.R. Slater; J. Mater. Chem. 19 (2009) 749.

9. S. Nakayama, H. Aono, Y. Sadaoka, Chem. Lett. (1995) 431.

10. S. Nakayama, M. Sakamoto, M. Higuchi, K. Kodaira; J. Mater. Sci. Lett. 19 (2000) 91.

11. H. Arikawa, H. Nishiguchi, T. Ishihara, Y. Takita, Solid State Ionics 136-137 (2000) 31.

12. J.E.H. Sansom, D. Richings, P.R. Slater, Solid State Ionics 139 (2001) 205.

13. L. Leon-Reina, M.C. Martin-Sedeno, E.R. Losilla, A. Cabeza, M. Martinez-Lara, S. Bruque, F.M.B. Marques, D.V. Sheptyakov, M.A.G. Aranda; Chem. Mater. 15 (2003) 2099.

14. L. Leon-Reina, E.R. Losilla, M. Martinez-Lara, S. Bruque, M.A.G. Aranda; J. Mater. Chem. 14 (2004) 1142.

15. J.R. Tolchard, M.S. Islam, P.R. Slater; J. Mater. Chem. 13 (2003) 1956.

16. V.V. Kharton, A.L. Shaula, M.V. Patrakeev, J.C. Waerenborgh, D.P. Rojas, N.P. Vyshatko, E.V. Tsipis, A.A. Yaremchenko, F.M.B. Marques; J. Electrochem. Soc. 151 (2004) A1236.

17. J.E.H. Sansom, J.R. Tolchard, D. Apperley, M.S. Islam, P.R. Slater; J. Mater. Chem. 16 (2006) 1410.

18. L. Leon-Reina, J.M. Porras-Vasquez, E.R. Losilla, M.A.G. Aranda; J. Solid State Chem. 180 (2007) 1250.

19. E. Rodriguez-Reyna, A.F. Fuentes, M. Maczka, J. Hanuza, K. Boulahya, U. Amador; Solid State Sci. 8 (2006) 168.

20. S. Celerier, C. Laberty-Robert, J.W. Long, K.A. Pettigrew, R.M. Stroud, D.R. Rolison, F. Ansart, P. Stevens, Adv. Mater., 18 (2006**)** 615.

21. S. S. Pramana, W.T. Klooster and T. J. White; Acta Cryst. B 63 (2007) 597.

22. A. Chesnaud, C. Bogicevic, F. Karolak, C. Estournes, G. Dezaneau; Chem. Commun. (2007) 1550.

23. J.R.Tolchard, J.E.H. Sansom, M.S. Islam, P.R. Slater; Dalton Trans. 7 (2005) 1273.

24. Y.V. Pivak, V.V. Kharton, A.A. Yaremchenko, S.O. Yakovlev, A.V. Kovalevsky, J.R. Frade, F.M.B. Marques, J. Euro Ceram Soc 27 (2007) 2445.

25. E. Kendrick, M.S. Islam, P.R. Slater; J. Mater. Chem. 17 (2007) 3104.

26. E. Kendrick, M.S.Islam, P.R. Slater; Chem. Commun (2008) 715.

27. A. Orera, E. Kendrick, D. C. Apperley, V.M. Orera, P.R. Slater; Dalton Trans. (2008) 5296.

28. J.E.H. Sansom, P.R. Slater; Solid State Ionics 167 (2004) 23.

29. H. Yoshioka; J. Amer. Ceram. Soc. 90 (2007) 3099.

30. E. Kendrick, P.R. Slater; Mater. Res. Bull. 43 (2008) 2509.

31. E. Kendrick, P.R. Slater; Solid State Ionics 179 (2008) 981.

32. P.J. Panteix, I. Julien, P. Abelard, D. Bernache-Assolant; Ceram. Int. 34 (2008) 1579.

33. T. Iwata, K. Fukuda, E. Bechade, O. Masson, I. Julien, E. Champion, P. Thomas; Solid State Ionics 178 (2008) 1523.

34. R. Ali, M. Yashima, Y. Matsushita, H. Yoshioka, K. Okoyama, F. Izumi; Chem. Mater. 20 (2008) 5203.

35. S.S. Pramana, W.T. Klooster, T.J. White; J. Solid State Chem. 181 (2008) 1717.

36. J.R. Tolchard, P.R. Slater; J. Phys. Chem. Solids 69 (2008) 2433.

37. A. Orera, P.R. Slater; Solid State Ionics (2009); doi 10.1016/j.ssi.2008.12.014

38. E. Kendrick, K.S. Knight, P.R. Slater; Mater. Res. Bull. 44 (2009) 1806.

39. J.M. Porras-Vazquez, E.R. Losilla, L. Leon-Reina, D. Marrero-Lopez, M.A.G. Aranda; J. Am. Ceram. Soc. 92 (2009) 1062.

40. C. Bonhomme, S. Beaudet-Savignat, T. Chartier, P-M. Geffroy, A-L. Sauvet ; J. Euro. Ceram. Soc. 29 (2009) 1781.

41. A. Al-Yasari, A. Jones, D.C. Apperley, D. Driscoll, M.S. Islam, P.R. Slater; J. Mater. Chem. 19 (2009) 5003.

42. E. Bechade, O. Masson, T. Iwata, I. Julien, K. Fukuda, P. Thomas, E. Champion; Chem. Mater. 21 (2009) 2508.

43. T. Baikie, P.H.J. Mercier, M.M. Elcombe, J.Y. Kim, Y. Le Page, L.D. Mitchell, T.J. White, P.S. Whitfield, Acta Crystallogr. B 63 (2007) 251.

44. S.J. Clarke, B.P. Guinot, C.W. Michie, M.J.C. Calmont, M.J. Rosseinsky; Chem. Mater. 14 (2002) 288.

Table 1. Compositions for $La_{8+x}Sr_{2-x}Si_6O_{26+x/2}$ samples after heating in ammonia at 600/800°C (compositions determined from thermogravimetric analysis).

x	Starting anion content	Temperature	Composition of oxynitride	Total anion content after NH_3 treatment
0	26.0	600°C	$La_8Sr_2Si_6O_{25.96(9)}N_{0.03(6)}$	25.99(3)
0.5	26.25	600°C	$La_{8.5}Sr_{1.5}Si_6O_{25.77(9)}N_{0.32(6)}$	26.09(3)
1.0	26.5	600°C	$La_9SrSi_6O_{26.02(9)}N_{0.32(6)}$	26.34(3)
0	26.0	800°C	$La_8Sr_2Si_6O_{25.96(9)}N_{0.03(6)}$	25.99(3)
0.5	26.25	800°C	$La_{8.5}Sr_{1.5}Si_6O_{25.26(9)}N_{0.66(6)}$	25.92(3)
1.0	26.5	800°C	$La_9SrSi_6O_{24.88(9)}N_{1.08(6)}$	25.96(3)

Table 2. Compositions for $La_{8+x}Sr_{2-x}Ge_6O_{26+x/2}$ samples after heating in ammonia at 600°C (compositions determined from thermogravimetric analysis).

x	Starting anion content	Composition of oxynitride	Total anion content after NH_3 treatment
0	26	$La_8Sr_2Ge_6O_{25.77(9)}N_{0.15(6)}$	25.92(3)
0.5	26.25	$La_{8.5}Sr_{1.5}Ge_6O_{25.08(9)}N_{0.78(6)}$	25.86(3)
1.0	26.5	$La_9SrGe_6O_{24.05(9)}N_{1.63(6)}$	25.68(3)
1.5	26.75	$La_{9.5}Sr_{0.5}Ge_6O_{24.09(9)}N_{1.77(6)}$	25.86(3)
2.0	27.0	$La_{10}Ge_6O_{24.04(9)}N_{1.97(6)}$	26.01(3)

Figure legends

Figure 1. X-ray diffraction patterns for $La_{8.5}Sr_{1.5}Si_6O_{26.25}$ before and after heating in NH_3 gas at 800°C, showing a slight shift in peaks on nitridation.

Figure 2. Variation in N content after heating $La_{8+x}Sr_{2-x}Si_6O_{26+x/2}$ samples in ammonia at 600/800°C.

Figure 3. ^{29}Si NMR data for $La_9SrSi_6O_{26.5}$ and $La_9SrSi_6O_{24.88(9)}N_{1.08(6)}$ showing a significant reduction in the peak shoulder at δ≈-80 ppm for the latter, along with evidence for a new shoulder at δ≈-73.5 ppm, consistent with the presence of a small amount of $[SiO_3N]^{5-}$

Figure 4. Nitridation process for an apatite silicate: (a) before, (b) after nitridation. During the process, $2N^{3-}$ replace $3O^{2-}$, leading to a loss of oxide ions from the interstitial sites, and the incorporation of N into the apatite channel sites.

Figure 5. X-ray diffraction patterns for $La_{10}Ge_6O_{27}$, before (lower) and after (upper) heating in NH_3 gas at 600°C, showing a change in symmetry from triclinic to hexagonal after NH_3 treatment.

Figure 6. Variation in N content after heating $La_{8+x}Sr_{2-x}Ge_6O_{26+x/2}$ samples in ammonia at 600°C.

Figure 1

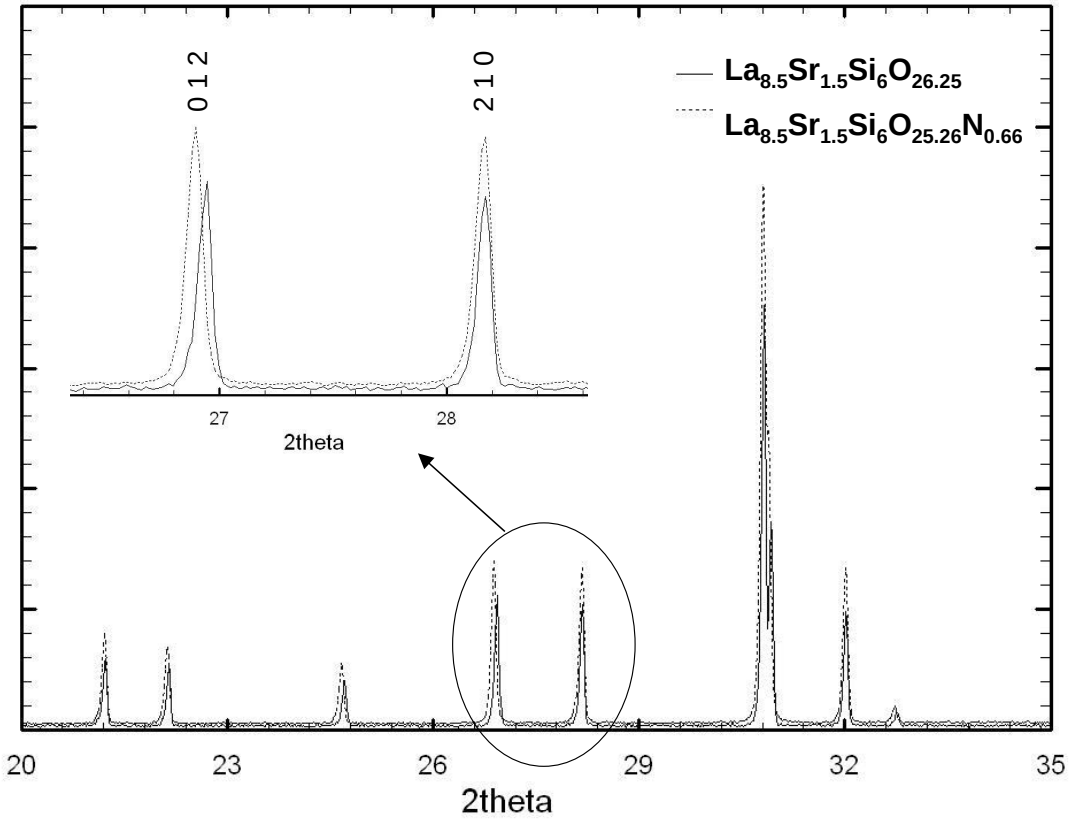
0 1 2
2 1 0
La8.5Sr1.5Si6O26.25
La8.5Sr1.5Si6O25.26N0.66
27
28
2theta
20
23
26
29
32
35
2theta

Figure 2.

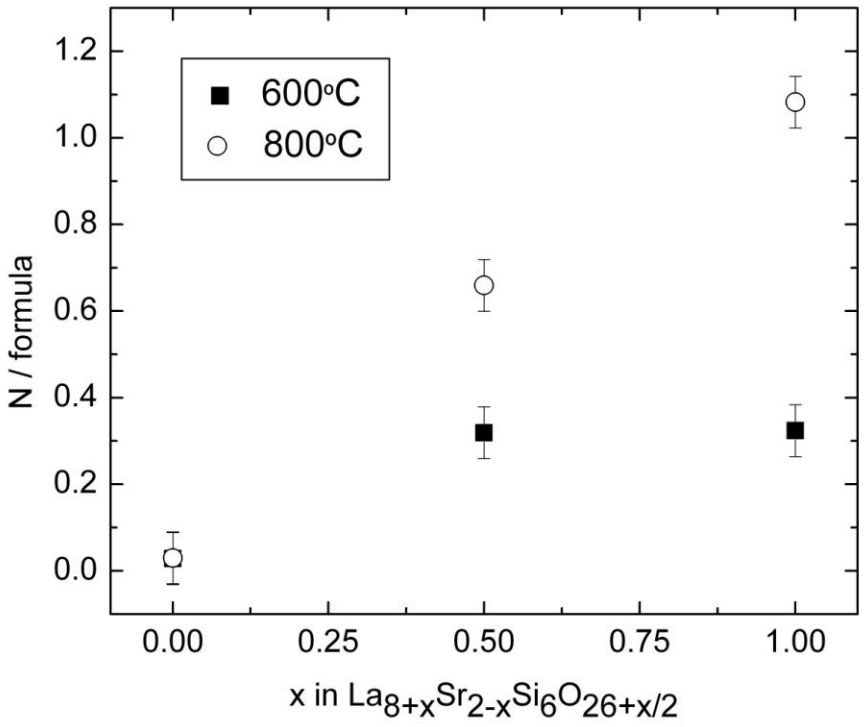
600°C
800°C
N / formula
1.2
1.0
0.8
0.6
0.4
0.2
0.0
0.00
0.25
0.50
0.75
1.00
x in La8+xSr2-xSi6O26+x/2

Figure 3.

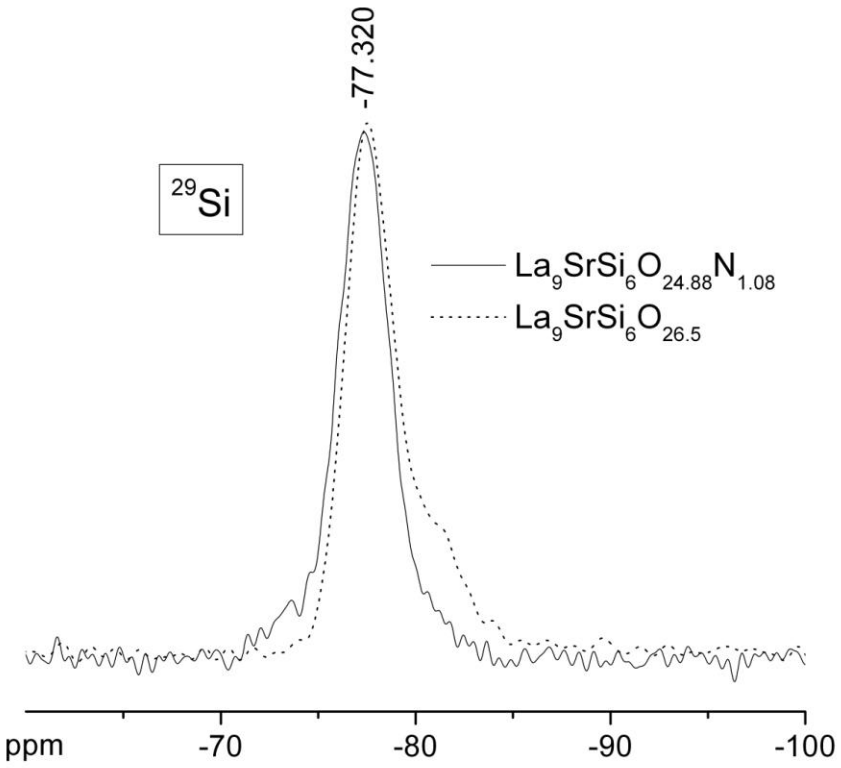
-77.320
^{29}Si
$La_9SrSi_6O_{24.88}N_{1.08}$
$La_9SrSi_6O_{26.5}$
ppm
-70
-80
-90
-100

Figure 4.

(a)

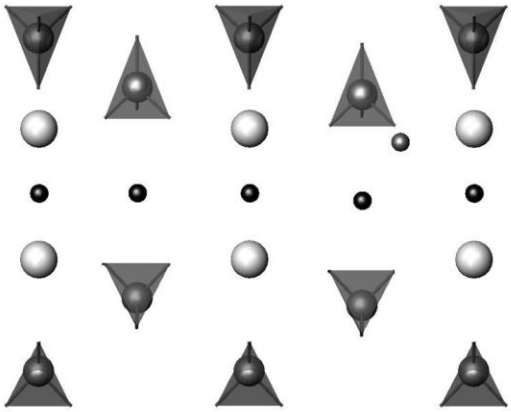

(b)

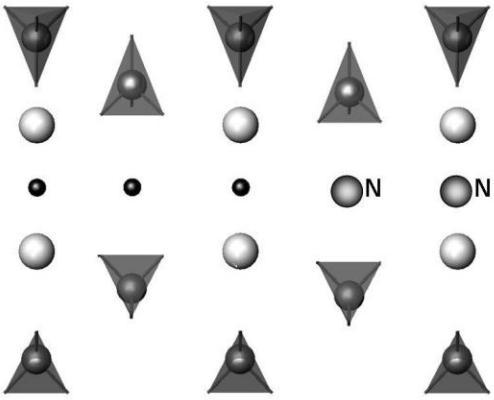

Figure 5.

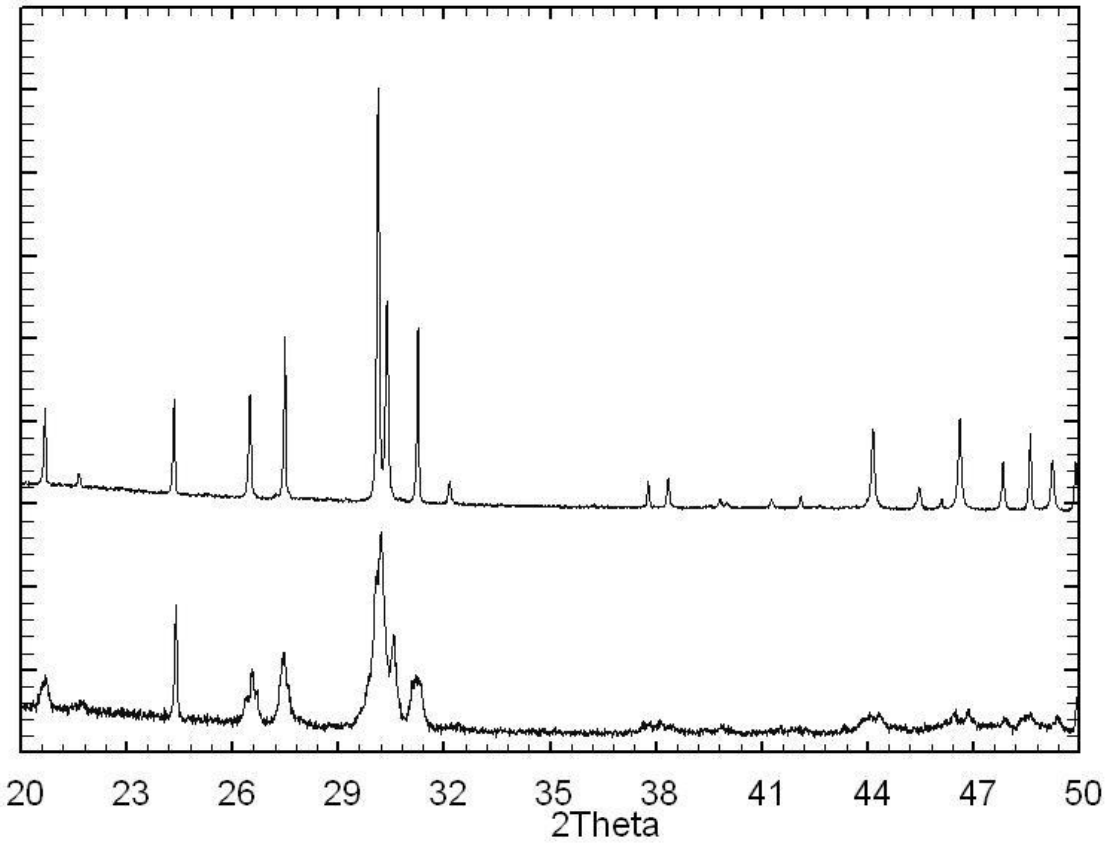

Figure 6.

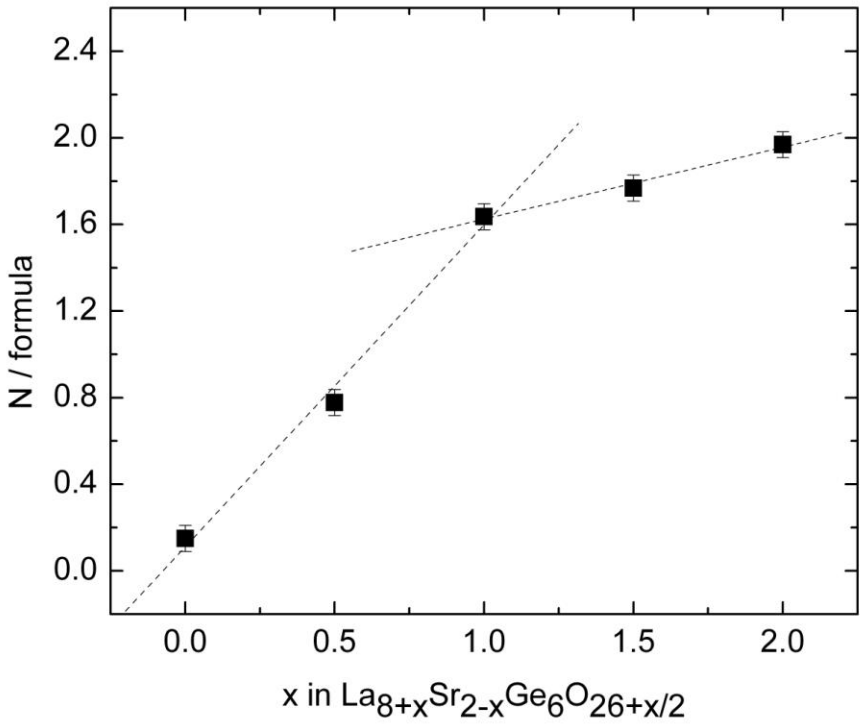
2.4
2.0
1.6
1.2
0.8
0.4
0.0
N / formula
0.0
0.5
1.0
1.5
2.0
x in La8+xSr2-xGe6O26+x/2